IOSR Journal of Applied Physics (IOSR-JAP)
e-ISSN: 2278-4861.Volume 18, Issue 1 Ser. 1 (Jan – Feb 2026), PP 85-92
www.iosrjournals.org

Characterization, Molecular dynamics simulation and Molecular Docking of Ethyl benzoate ($C_9H_{10}O_2$)

Tanveer Hasan [#a]
[a]*Deptt. of Physics, Shia P.G. College, Lucknow-226020, India.*

Abstract
Present study is based on the investigation of molecular dynamics and molecular docking analysis in detail of the title molecule entitled with "Ethyl benzoate ($C_9H_{10}O_2$) " [ETBEN] bearing anticarcinogenic effect using quantum computational method. A molecular dynamics simulation of 100 ns was performed, assessing models through RMSD, RMSF, Rg, PC1-PC2-PLOT metrics, and the MMPBSA/MMGBSA tool was employed for calculating free energy. The proteins 1W7C and 5XNW have undergone molecular docking analysis with the title molecule ETBEN to examine the possible bioactive properties.

Keywords: *Ethyl benzoate, [$C_9H_{10}O_2$], Molecular dynamics simulations; DFT; Molecular Dynamics simulation.*

I. Introduction

Ethyl benzoate [ETBEN] is a type of benzoate ester made when benzoic acid reacts with ethanol. Plants biosynthesize ethyl benzoate as a volatile secondary metabolite. It occurs naturally in kiwifruit, cranberries, apples, bananas, cherries, and black tea [1]. Alkyl chain length in benzoate esters influences bioactivity against microorganisms. Ethyl benzoate provides functional inhibition properties used in specific industrial and cosmetic formulations[2]. The compound's equilibrium geometry has been derived and examined using the DFT-B3LYP/LANL2DZ approach using Gaussian 09 software. The model molecular structure was obtained employing Gaussview 6.0. Molecular dynamics (MD) simulations investigate the time-dependent physical, structural, and thermodynamic properties of chemical drugs and their interactions with biological targets [3]. For the study of antimicrobial and other bioactive properties, we have also performed a molecular docking analysis of the ligand NPU with two proteins 1W7C and 5XNW.

II. Computational details

Gaussian 09 software was used to perform quantum chemical calculations for the studied molecule ETBEN [4]. The model molecular structure of the compound was produced employing Gaussview 6 [5]. In this work, DFT is used in conjunction with the Lee, Yang, and Parr correlation functional and Becke's three-parameter hybrid exchange functional B3LYP [6-8]. The Schrödinger's molecular dynamics software (Desmond) platform was used for all of the molecular dynamics simulations [9]. Molecular Docking calculations were conducted using Autodock Vina tools 4.2.6 [10] and Discovery Studio.

III. Results and Discussion

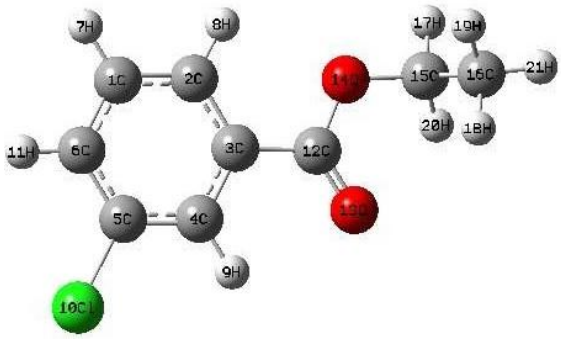

Fig.-1: Model molecular structure of ETBEN as produced by GaussView 6 software

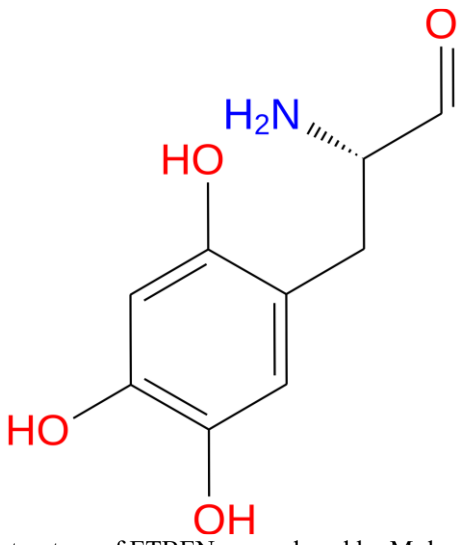

Fig.-2 : Model molecular structure of ETBEN as produced by Molecular Dynamics Simulation

Figure 1 shows the title compound's ETBEN optimal configuration produced from the Gauss View 6, whereas figure 2 is obtained from the molecular dynamics simulations.

3.1 Molecular Dynamics Simulations

3.1.1 RMSD Analysis

The root mean square deviation (RMSD) technique was employed to examine the structural behavior of ligands in the active region of proteins. Figure 3(a) and (b) display the RMSD plots for the examined ligand, ETBEN, in relation to the two protein receptors, 1W7C and 5XNW, respectively. It is obtained that for ETBEN-1W7C and ETBEN-5XNW ligand-protein receptor combinations RMSD value for proteins 1W7C, and 5XNW (in blue color) initially rises from 0.6 Å to 4.2 Å then fluctuates between 3.25 to 5.4 Å and it finally stabilized at nearly 4.5 Å. For ligand ETBEN, RMSD fluctuation starts from 0.6 Å fluctuates between 5.4 and 4.2 Å before finally stabilizing at 4.5 Å . For the ETBEN-5XNW, combination, the value of RMSD for the protein receptor 5XNW starts from 0.6 Å, peaks at σ =2.40 Å and fluctuates between 2.4 and 0.6 Å before finally settling at 1.2 Å at 100 ns.

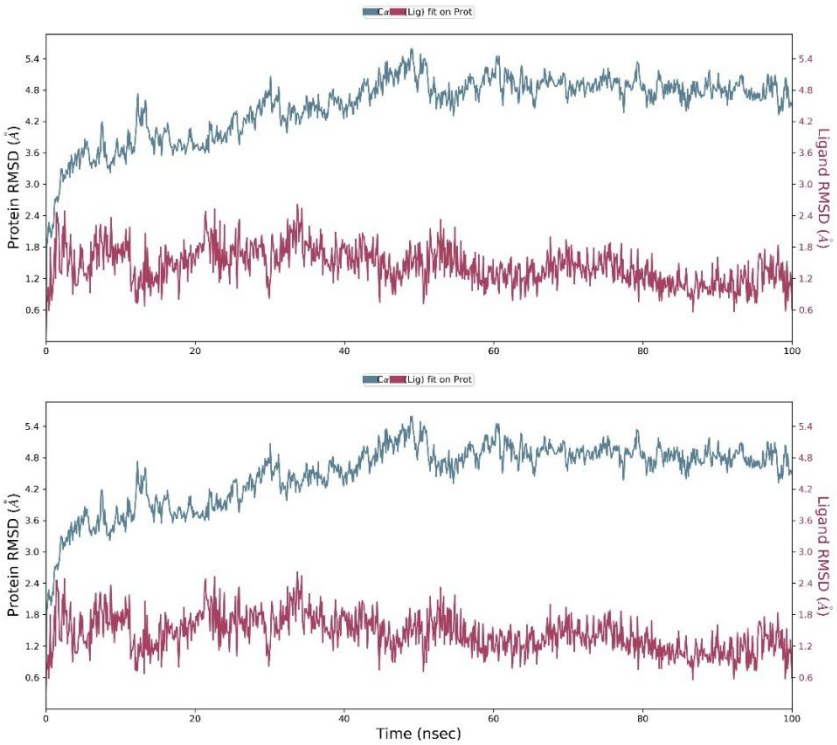

Fig.-3: RMSD fluctuations of ETBEN with the two-protein receptor

3.1.2 Root Mean Square Fluctuations

Figure 4(a) and (b) display the root mean square (RMS) fluctuations of the title molecule ETBEN interacting with the two receptor proteins, 1W7C and 5XNW, respectively. The graphical data suggest that the RMS fluctuations are highest with the value reaching to 7.2 Å near the residue index with 68-690 atoms, for both the receptors. Both protein receptors exhibit similar structural behavior influenced by the ligand ETBEN, resulting in comparable contributions to their RMS fluctuations. Ligand RMSF shows the ligand's fluctuations broken down by atom, corresponding to the 2D structure in the top panel. The ligand RMSF may give you insights on how ligand fragments interact with the protein and their entropic role in the binding event. In the bottom panel, the 'Fit Ligand on Protein' line shows the ligand fluctuations, with respect to the protein. The protein-ligand complex is first aligned on the protein backbone and then the ligand RMSF is measured on the ligand heavy atoms.

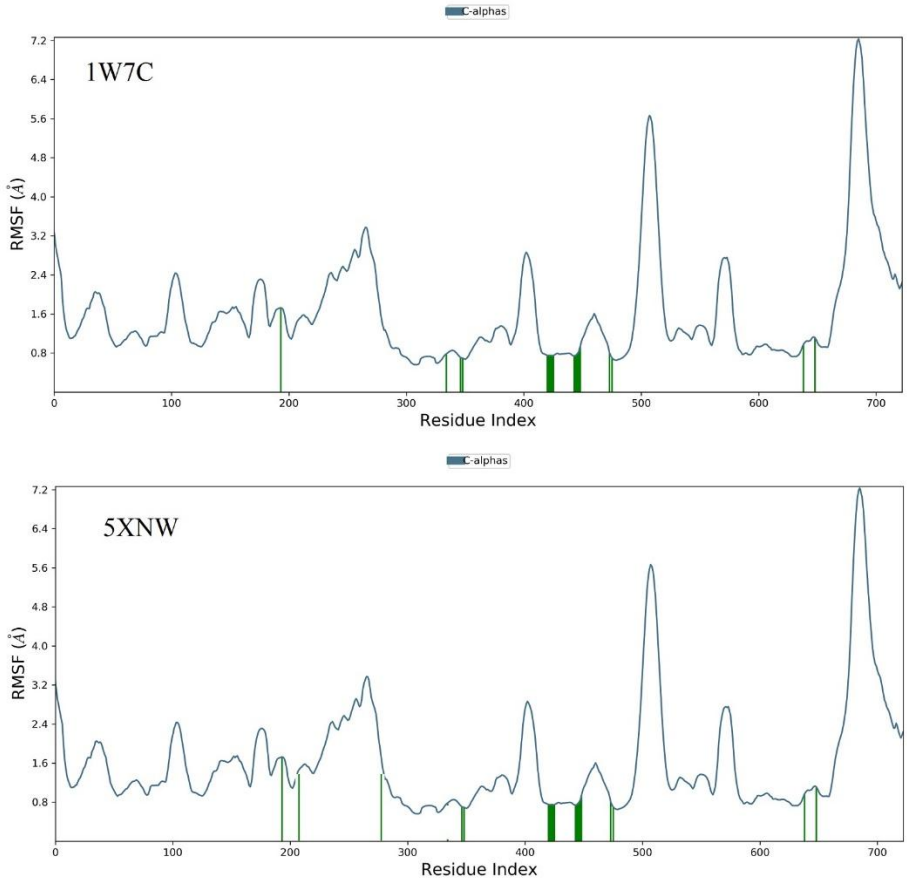

Fig.-4: RMSF fluctuations of ligand with the two-protein receptor

3.1.3 Radius of Gyration (R_g)

The radius of gyration (Rg) can be used to calculate the structural compactness of a protein structure. The graphical representations of Rg can help assess the rigidity level of a protein structure. Throughout the 100 ns simulation duration, well-folded proteins show relatively stable values, while misfolded or unstable proteins display variations. The 2D plots in figures 5(a) and (b) indicate that Rg fluctuated until 95 ns, at which point the Rg values for the protein receptors 1W7C and 5XNW became stable at 2.92 Å due to the ligand ETBEN.

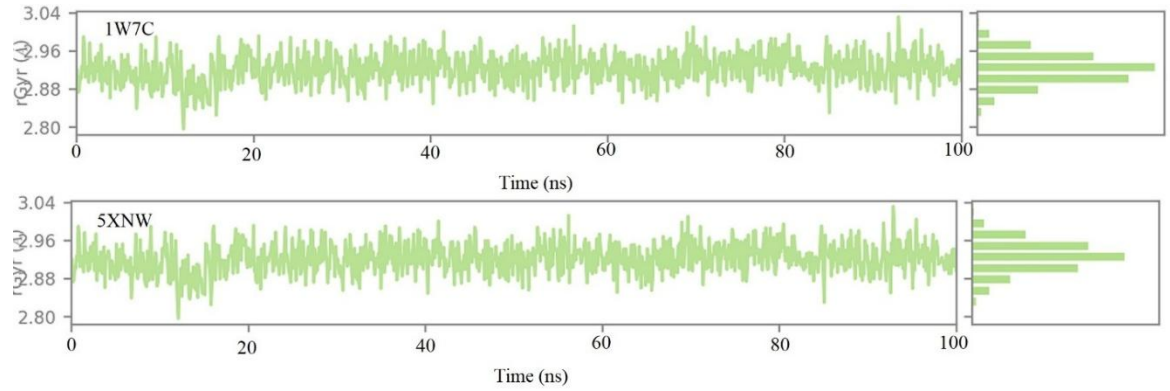

Fig. 5: Radius of gyration (Rg) fluctuations of ligand with the two-protein receptor

3.1.4 PC1 and PC2 projections

Principal component analysis is commonly utilized as a method in exploratory data analysis to uncover the underlying data structure in a manner that most effectively elucidates its variance. When applied to a collection of snapshots from an MD trajectory, the PCs illustrate collective atomic movements and can emphasize significant conformational alterations between the structures [11,12]. Figures 6(a) and (b) show two-dimensional projections of PC1 and PC2 for the ligand ETBEN with the proteins 1W7C and 5XNW over the duration of 100 ns MD simulations. The green hue signifies anti-correlated movement, whereas the pastel shade indicates correlated movement. These images clearly show that the PC1 Vs PC2 projections are identical for both protein receptors.

3.1.5 Protein -Ligand Contacts

Protein interactions with the ligand can be monitored throughout the simulation. These interactions can be categorized by type and summarized, as shown in the plot above. Protein-ligand interactions (or 'contacts') are categorized into four types: Hydrogen Bonds, Hydrophobic, Ionic and Water Bridges. Each interaction type contains more specific subtypes, which can be explored through the 'Simulation Interactions Diagram' panel. The stacked bar charts are normalized over the course of the trajectory: for example, a value of 0.7 suggests that 70% of the simulation time the specific interaction is maintained. Values over 1.0 are possible as some protein residue may make multiple contacts of same subtype with the ligand.

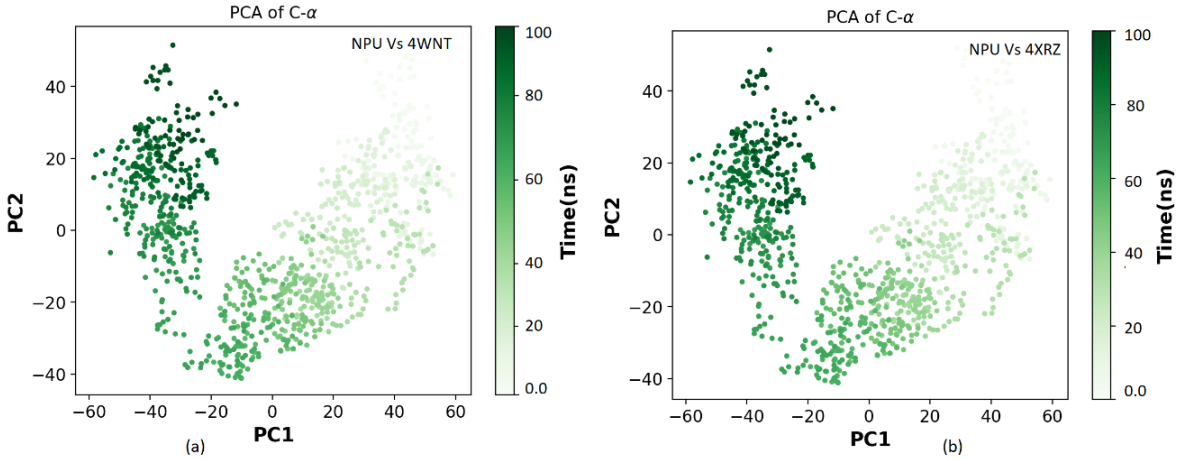

Fig. 6. 2D-Projection's trajectories PC1 & PC2 of ETBEN with the protein receptors (a) 1W7C and (b) 5XNW

Hydrogen Bonds: (H-bonds) play a significant role in ligand binding. Consideration of hydrogen-bonding properties in drug design is important because of their strong influence on drug specificity, metabolization and adsorption. Hydrogen bonds between a protein and a ligand can be further broken down into four subtypes: backbone acceptor; backbone donor; side-chain acceptor; side-chain donor. The current geometric criteria for protein-ligand H-bond is: distance of 2.5 Å between the donor and acceptor atoms (D—H···A); a donor angle of $^{3}120°$ between the donor-hydrogen-acceptor atoms (D—H···A); and an acceptor angle of $^{3}90°$ between the hydrogen-acceptor-bonded-atoms (H···A—X).

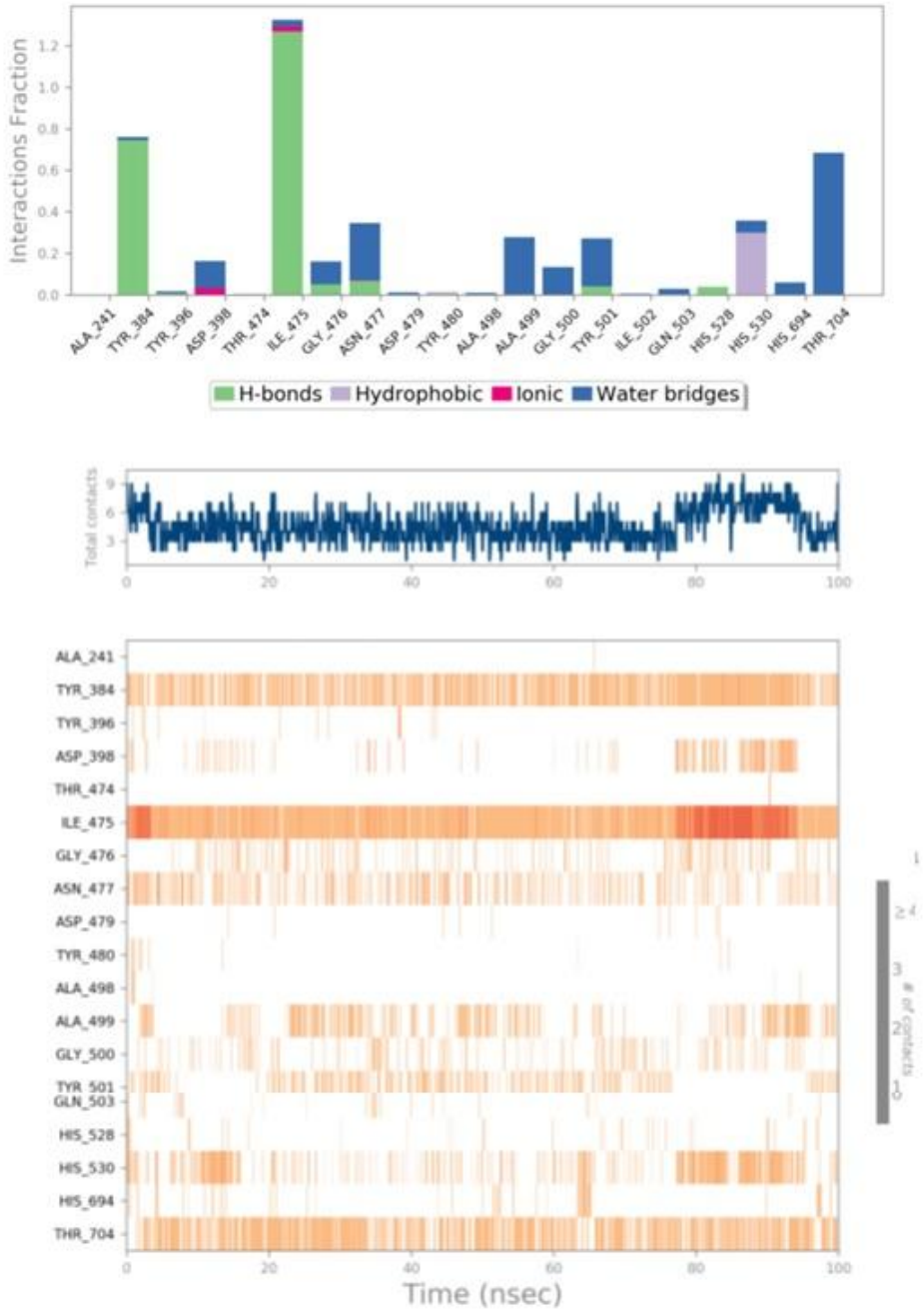

Fig. 7: Ligand-protein-contacts-with residues number

Hydrophobic contacts: fall into three subtypes: p-Cation; p-p; and Other, non-specific interactions. Generally, these types of interactions, involve a hydrophobic amino acid and an aromatic or aliphatic group on the ligand, but we have extended this category to also include p-Cation interactions. The current geometric criteria for hydrophobic interactions is as follows: p-Cation — Aromatic and charged groups within 4.5 Å; p-p — Two aromatic groups stacked face-to-face or face-to-edge; Other — A non-specific hydrophobic sidechain within 3.6 Å of a ligand's aromatic or aliphatic carbons.

Ionic interactions: or polar interactions, are between two oppositely charged atoms that are within 3.7 Å of each other and do not involve a hydrogen bond. We also monitor Protein-Metal-Ligand interactions, which are defined by a metal ion coordinated within 3.4 Å of protein's and ligand's heavy atoms (except carbon). All ionic interactions are broken down into two subtypes: those mediated by a protein backbone or side chains.

Water Bridges: are hydrogen-bonded protein-ligand interactions mediated by a water molecule. The hydrogen-bond geometry is slightly relaxed from the standard H-bond definition.
The current geometric criteria for a protein-water or water-ligand H-bond are: a distance of 2.8 Å between the donor and acceptor atoms (D—H···A); a donor angle of ³110° between the donor-hydrogen-acceptor atoms (D—H···A); and an acceptor angle of ³90° between the hydrogen-acceptor-bonded-atom atoms (H···A—X).

3.1.6 Ligand-Protein Contacts
A schematic of detailed ligand atom interactions with the protein residues in figure 6. Interactions that occur more than20.0% of the simulation time in the selected trajectory (0.00 through 100.00 ns), are shown. It is possible to have interactions with >100% as some residues may have multiple interactions of a single type with the same ligand atom. For example, the ARG side chain has four H-bond donors that can all hydrogen-bond to a single H-bond acceptor.
3.1.7 Solvent Accessible Surface Area (SASA)
It gives the information about surface area of a molecule accessible by a water molecule. The SASA schematic of the ligand ETBEN with two proteins are shown in figure 9. The SASA values varies between 0.5 to 30 before finally stabilizing at approximately 20 Å^2.

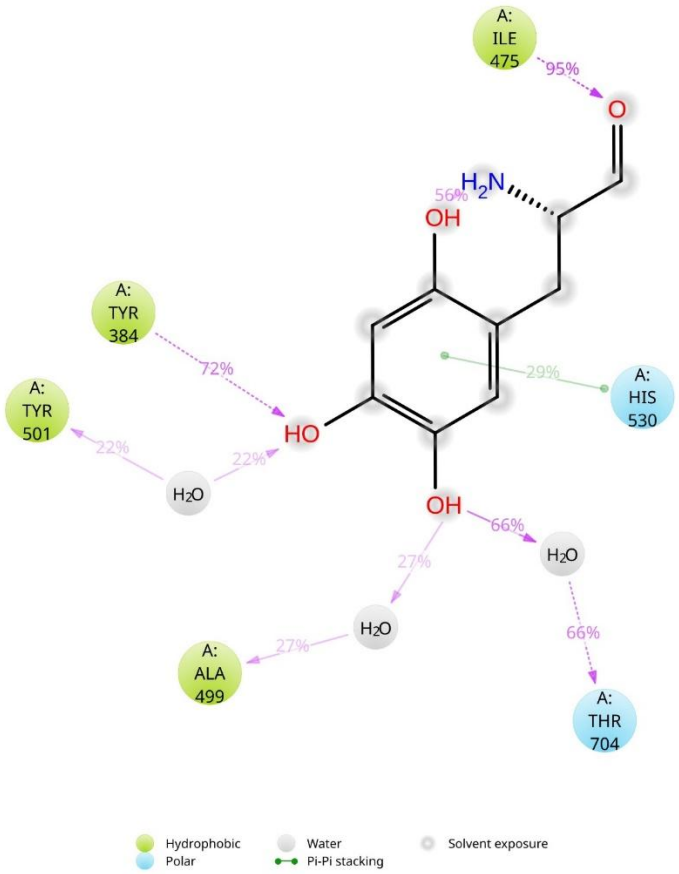

Fig. 8: Ligand-protein-contacts-with residues distances

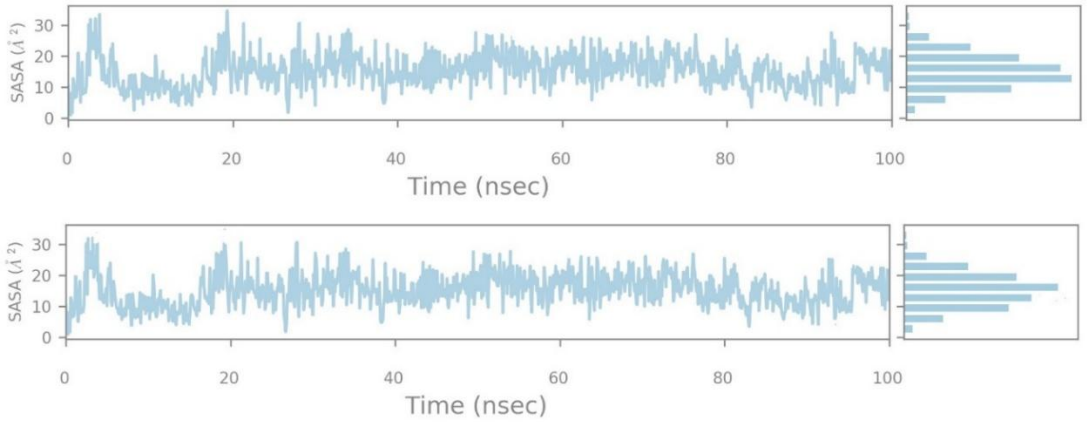

Fig. 9: SASA of the ligand ETBEN with two proteins

3.2 Molecular docking

For docking analysis, the target proteins were selected using the way2drug.com online target prediction tool [13]. The proteins of focus (PDB ID: "1W7C and 5XNW") were obtained from the Protein Data Bank [14]. The selected protein receptor was the Peroxisome proliferator-activated receptor gamma, Cytochrome P450 4A11 etc.

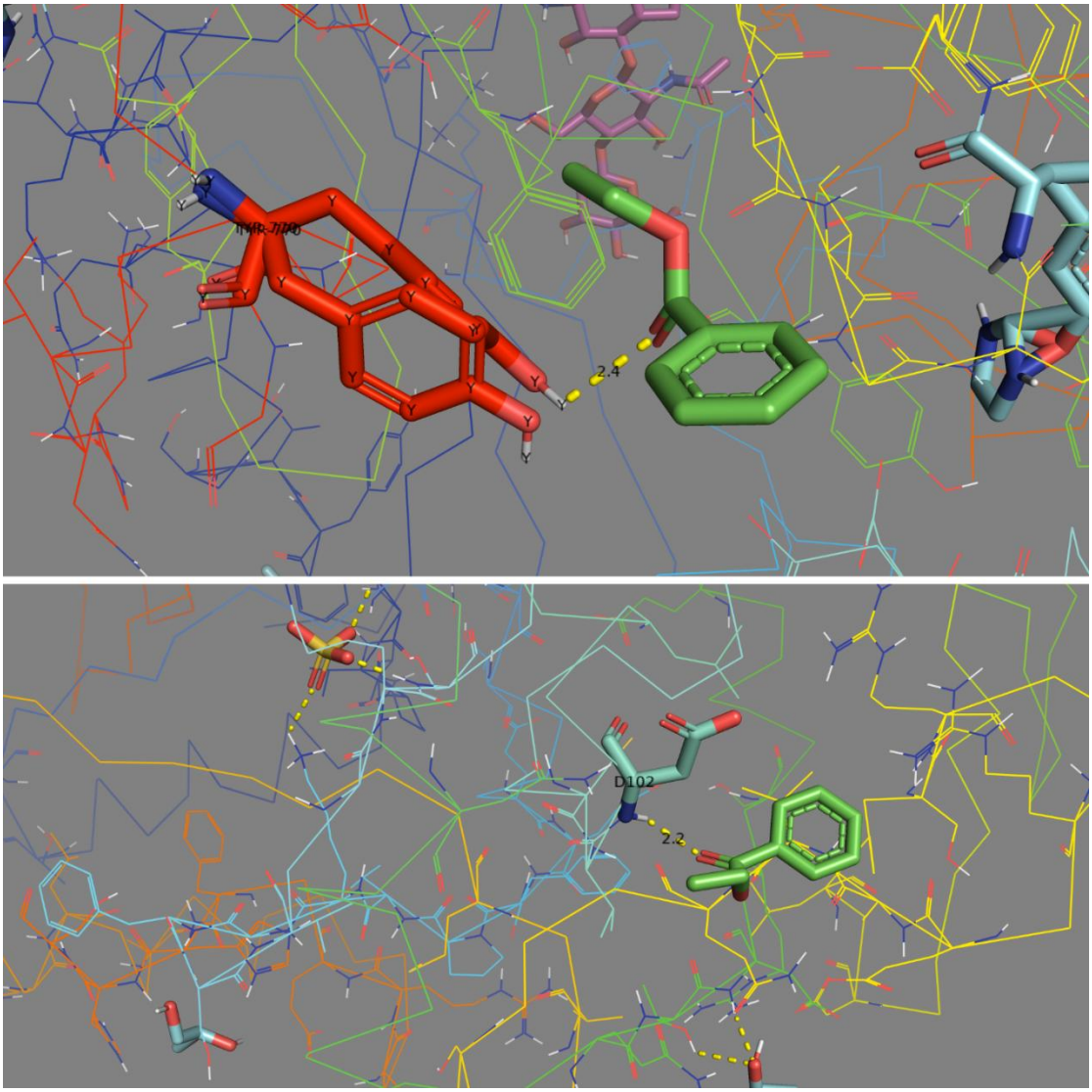

Fig. 10: Molecular docking poses as obtained by PyMol software

The proteins, ligands, and grid maps were prepared for docking with Auto Grid and Auto Dock tools, and docking calculations were carried out using the Autodock Vina 4.2.6 software. 2D interaction profile images of the ligand NPU with proteins 1W7C and 5XNW were created using PYMOL software [15, 16]. Analysis of docking in PYMOL for ETBEN with the 1W7C protein receptor indicated one hydrogen bond with the residue TYR-770 at distances of 2.4 Å, exhibiting an interaction energy of -6.2 Kcal/mol. When these interactions were analyzed through Discovery Studio software [17, 18], only one hydrogen bond was found: involving the TYR-312 residue at distances of 2.42 Å for ETBEN-1W&C complex. Similarly, the analysis of docking for ETBEN with the 5XNW protein receptor indicated one hydrogen bond with the residue D102 at distances of 2.2 Å, exhibiting an interaction energy of -4.2 Kcal/mol.

IV. Conclusions

A theoretical quantum chemical investigation of Ethyl benzoate (C9H10O2) [ETBEN] was conducted using the DFT-B3LYP/LANL2DZ approach. Molecular dynamics simulations showed that the ligand ETBEN has been performed to assess RMSD, RMSF, Rg, PC1 & PC2, along with interaction energies, are almost identical for the two ligand-protein complexes. Identical Receptor Fluctuation Profiles: Both protein receptors (1W7C and 5XNW) exhibit nearly identical structural flexibility patterns when interacting with the ligand ETBEN. This is highlighted by matching, pronounced peak fluctuations reaching 7.2 Å at the specific residue region (index 68–690), demonstrating that ETBEN drives uniform local dynamics across both systems. The identical PC1 and PC2 projections for the ligand ETBEN with proteins 1W7C and 5XNW indicate that both receptors undergo highly conserved collective atomic movements and share structurally analogous essential dynamics over the 100 ns trajectory. The Radius of Gyration analysis demonstrates that the ligand ETBEN induces identical structural stabilization in protein receptors 1W7C and 5XNW, with values converging to a stable 2.92 Å after 95 ns. This conformational tightening is supported by a robust, persistent network of protein-ligand contacts that maintains structural rigidity throughout the trajectory. Molecular docking results indicated that the ETBEN-5XNW complex exhibited the strongest docking with an interaction energy of -6.8 Kcal/Mol, in contrast to ETBEN-5XNW, which had an interaction energy of -6.3 Kcal/Mol.

These findings demonstrate that ETBEN exerts a uniform mechanical effect and drives equivalent conformational adaptation pathways across both protein systems. These findings may lead to the development of additional new biologically active compounds that contain Ethyl benzoate rings.

References

[1] https://pubchem.ncbi.nlm.nih.gov/compound/Ethyl-benzoate
[2] https://www.benchchem.com/product/b195668.
[3] Salo-Ahen, Outi M. H., Ida Alanko, Rajendra Bhadane, Alexandre M. J. J. Bonvin, Rodrigo Vargas Honorato, Shakhawath Hossain, André H. Juffer, Aleksei Kabedev, Maija Lahtela-Kakkonen, Anders Støttrup Larsen, and et al. 2021. Processes 9, no. 1: 71. https://doi.org/10.3390/pr9010071.
[4] Frisch, M. J.; Trucks, G. W.; Schlegel, H. B.; Scuseria, G.E.; Robb, M. A.; Cheeseman, J. R.; Montgomery, Jr., J.A.; Vreven, T.; Kudin, K. N.; Burant, J. C.; Millam, J. M.; Iyengar, S. S.; Tomasi, J.; Barone, V.; Mennucci, B.; Cossi, M.; Scalmani, G.; Rega, N.; Petersson, G. A.; Nakatsuji, H.; Hada, M.; Ehara, M.; Toyota, K.; Fukuda, R.; Hasegawa, J.; Ishida, M.; Nakajima, T.; Honda, Y.;Kitao, O.; Nakai, H.; Klene, M.; Li, X.; Knox, J. E.; P. Hratchian, H.; Cross, J. B.; Adamo, C.; Jaramillo, J.; Gomperts, R.; Stratmann, R. E.; Yazyev, O.; Austin, A. J.; Cammi, R.; Pomelli, C.; Ochterski, J. W.; Ayala, P. Y.; Morokuma, K.; Voth, G. A.; Salvador, P.; Dannenberg, J. J.; Zakrzewski, V. G.; Dapprich, S.; Daniels, A. D.; Strain,M. C.; Farkas, O.; Malick, D. K.; Rabuck, A. D.; Raghavachari, K.; Foresman, J. B.; Ortiz, J. V.; Cui, Q.; Baboul, A. G.; Clifford, S.; Cioslowski, J.; Stefanov, B. B.; Liu, G.; Liashenko, A.; Piskorz, P.; Komaromi, I.; Martin,
R. L.; Fox, D. J.; Keith, T.; Alâ€Laham, M. A.; Peng, C. Y.; Nanayakkara, A.; Challacombe, M.; Gill, P. M. W.; Johnson, B.; Chen, W.; Wong, M. W.; Gonzalez, C.; Pople, J. A. et al., Gaussian 09, revision A. 02, Gaussian, Inc., Wallingford CT, 2009.
[5] Frisch, A. et al. Gaussian Inc. GaussView, Version 6; 2009.
[6]. Becke, A.D. J. Chem. Phys. 1993, 98, 5648.
[7]. Hohenberg, P.; Kohn, W. Phys. Rev. B. 1964, 136, 864.
[8]. Lee, C.; Yang, W.; Parr, R. G. Phys. Rev. B. 1988, 37, 785.
[9]. Jacobson, L.D.; Bochevarov, A. D.; Watson, M. A.; Hughes, T. F.; Rinaldo, D.; Ehrlich, S.; Steinbrecher, T. B.; Vaitheeswaran, S.; Philipp, D. M.; Halls, M. D.; Friesner, R. A., "Automated Transition State Search and Its Application to Diverse Types of Organic Reactions", J. Chem. Theory Comput. 2017, 13(11), 5780–5797.
[10]. Trott, O.; Olson, A. J. J. Comp. Chem. 2010, 31, 455.
[11]. Papaleo E, Mereghetti P, Fantucci P, Grandori R, Gioia LD, J Mol Graph Model, 27:889–899, (2009).
[12]. Valdés-Tresanco, M. S.; Valdés-Tresanco, M. E.; Valiente, P. A.; Moreno, E. J. Chem. Theory Comput. 17, 6281, 2021.
[13]. Lange O. F., Grubmüller H, *J. Phys. Chem. B*. 110:22842–22852, (2006).
[14]. Papaleo E, Mereghetti P, Fantucci P, Grandori R, Gioia LD, *J Mol Graph Model*, 27:889–899, (2009).
[15]. Valdés-Tresanco, M. S.; Valdés-Tresanco, M. E.; Valiente, P. A.; Moreno, *E. J. Chem. Theory Comput.* 17, 6281, 2021.
[16]. Rudik A., Dmitriev A., Lagunin A., Filimonov D., Poroikov V. *Bioinformatics*, 31 (12), 2046-2048 (2015).
[17]. Fusion protein of heme oxygenase-1 and NADPH cytochrome P450 reductase (17aa). Available at: http://www.rcsb.org/pdb/explore.do?structureId=6J7 A&6J7I
[18]. Morris, G. M.; Huey, R.; Lindstrom, W.; Sanner, M. F.; Belew, R. K.; Goodsell, D. S.; Olson, A. J. *J. Comput. Chem.* 2009, 16, 2785.